Journal of Physiology (1993), **463**, *pp.* 689–707
With 8 figures
Printed in Great Britain

CALCIUM TRANSIENTS IN SINGLE MAMMALIAN SKELETAL MUSCLE FIBRES

BY O. DELBONO AND E. STEFANI

From the Department of Molecular Physiology and Biophysics, Baylor College of Medicine, Houston, TX 77030, USA

(*Received 24 March 1992*)

SUMMARY

1. We studied the transient changes in myoplasmic Ca^{2+} concentration under current- and voltage-clamp (double Vaseline-gap technique) in cut fibres of rat extensor digitorum longus muscle using mag-fura-2 (furaptra) as Ca^{2+} indicator, at 3·6–3·8 μm sarcomere length and 17 °C. Mag-fura-5 and fura-2 were also used in order to characterize some aspects of the Ca^{2+} transients.

2. The peak [Ca^{2+}] in response to a single action potential was $4·6 \pm 0·4$ μM ($n = 5$). The time to peak of the Ca^{2+} transient was $4·6 \pm 0·42$ ms, with half-width of $8·2 \pm 1·5$ ms, time constant of the rising phase $1·15 \pm 0·25$ ms, time constant of the decaying phase $3·26 \pm 0·65$ ms, and delay between action potential and Ca^{2+} transient $2·0 \pm 0·2$ ms.

3. Ca^{2+} transients were studied under voltage-clamp conditions at different voltages and pulse durations. The rising phase showed a complex temporal course with a fast initial increase and a second component. Both components were separated by a plateau or a brief decrease of the Ca^{2+} concentration. The peak Ca^{2+} transient was $10·5 \pm 1·3$ μM ($n = 22$).

4. After interrupting the pulse, Ca^{2+} concentration decayed exponentially. The time constant of decay of the Ca^{2+} transient increased with the pulse voltage and duration, reaching a maximum value at potentials more positive than +10 mV and pulses longer than 200 ms. An analysis of the decaying phases of the Ca^{2+} transients suggests that only the removal process operates after fibre repolarization.

5. The rate of Ca^{2+} release from the sarcoplasmic reticulum was calculated using the Melzer, Ríos & Schneider model. The value of $17·2 \pm 3·1$ μM ms^{-1} ($n = 10$) estimated in these calculations was intermediate between those obtained by other authors from cut frog muscles (10 μM ms^{-1}) and intact frog fibres (100 μM ms^{-1}) using antipyrylazo III (AP III) as the Ca^{2+} indicator.

INTRODUCTION

Most of the information about the transient changes in myoplasmic Ca^{2+} concentration as a consequence of sarcolemmal depolarization comes from amphibian muscle using different low-affinity metallochromic Ca^{2+}-sensitive dyes: arsenazo III and antipyrylazo III (AP III), and purpurate dyes: tetramethylmurexide and

purpurate-3,3'diacetic acid (PDAA) (Miledi, Parker & Schalow, 1977, 1981; Kovács, Ríos & Schneider, 1979; Hirota, Chandler, Southwick & Waggoner, 1989; Konishi & Baylor, 1991). Ca^{2+} signals were further characterized by the simultaneous use of the relatively low-affinity (antipyrylazo III) and high-affinity (fura-2) Ca^{2+} indicators in the same intact or cut single muscle fibre (Baylor & Hollingworth, 1988; Klein, Simon, Szücs & Schneider, 1988). Due to inherent technical difficulties, Ca^{2+} transients from mammalian skeletal muscle fibres were not extensively studied. Eusebi, Miledi & Takahashi (1980, 1985) studied Ca^{2+} transients in extensor digitorum longus, soleus and diaphragm muscle fibres with the photoprotein aequorin. Recently García & Stefani (1990) and García & Schneider (1992) in two short communications described some aspects of the Ca^{2+} transients in mammalian fibres with AP III using the double Vaseline-gap technique.

Konishi, Hollingworth, Harkins & Baylor (1991) recently recorded frog skeletal muscle Ca^{2+} transients with mag-fura-2 (furaptra), which is a low-affinity Ca^{2+} indicator (Raju, Murphy, Levy, Hall & London, 1989). According to Konishi *et al.* (1991), mag-fura-2 has some advantages compared with AP III, such as 1:1 stoichiometry for dye–Ca^{2+} complex, fast diffusion inside the cell, less binding to fibre components, and less interference from fibre contraction (mechanical artifact) on fluorescence records. These properties prompted us to study Ca^{2+} transients with mag-fura-2 in mammalian single fibres of 3·6–3·8 μm sarcomere length. Furthermore, we characterized Ca^{2+}-transient kinetics using relatively low-affinity (mag-fura-5) and high-affinity (fura-2) Ca^{2+} indicators which have the same excitation and emission spectrum as mag-fura-2.

Part of this work has already been presented elsewhere (Delbono & Stefani, 1992).

METHODS

Fibre preparation. Single fibres from extensor digitorum longus (EDL) muscle of the rat were manually dissected and mounted following previous procedures (Delbono, García, Appel & Stefani, 1991; Delbono, 1992). Briefly extensor digitorum longus (EDL) muscle was dissected after the rat was killed in a carbon dioxide chamber. The muscles were kept for 8–9 h in a beaker containing a modified Krebs solution. In most of the experiments, fibres were stretched to 3·6–3·8 μm sarcomere length.

Solutions. Action potentials were recorded in external modified Krebs solution (mM): 145 NaCl, 5 KCl, 2·5 $CaCl_2$, 1 $MgSO_4$, 10 Hepes-Na, 10 glucose. The external solution for voltage-clamp experiments contained (mM): 150 TEA-$MeSO_3$ (tetraethylammonium-methanesulphonic acid), 2 $CaCl_2$, 2 $MgCl_2$, 2 TEA-Hepes (*N*-2-hydroxyethylpiperazine-*N'*-2-ethanesulphonic acid) and 0·001 TTX (tetrodotoxin), 1 anthracene-9-carboxylic acid, and 1 3,4-diaminopyridine (pH adjusted to 7·2 with TEAOH). The internal solution contained (mM): 98 potassium glutamate, 0·1 K_2-EGTA, 0·0082 $CaCl_2$, 5 Na_2ATP, 5·5 $MgCl_2$, 5 glucose, 5 K-Hepes, 5 creatine phosphate (disodium salt), pH 7·2. The osmolarity of the solutions was 300 mosmol l^{-1}. Mag-fura-2, mag-fura-5 and fura-2 (Molecular Probes, Inc., Eugene, OR, USA) were added from 5 mM stock solutions (in deionized water) to final concentrations of 100–400, 100 and 50 μM respectively. Free Ca^{2+} and Mg^{2+} concentrations in solutions were calculated according to Fabiato (1988).

Set-up. Figure 1 shows a muscle fibre positioned in a lucite chamber. The two central Vaseline seals produce three compartments: one central (extracellular) and two lateral pools (intracellular). Sarcomere length, fibre diameter, width of the seals and width of the central pool were measured by transillumination with a tungsten–halogen lamp (not shown in the diagram). Both ends were clamped with small sliding glass pieces. Small transversal cuts were made to the fibre close to both seals in the lateral pools. Fibres were voltage clamped using the double Vaseline-gap technique similar to the one introduced by Kovács, Ríos & Schneider (1983) and modified by Francini &

Stefani (1989) at a holding potential of −80 mV. Temperature was monitored with a thermistor probe positioned close to the fibre in the middle pool. The transmittance characteristics of all optical components were determined with a spectrophotometer (Hewlett Packard 8452A Diode Array, UV/VIS, Palo Alto, CA, USA). For fluorescent recordings, the fibre was epi-illuminated

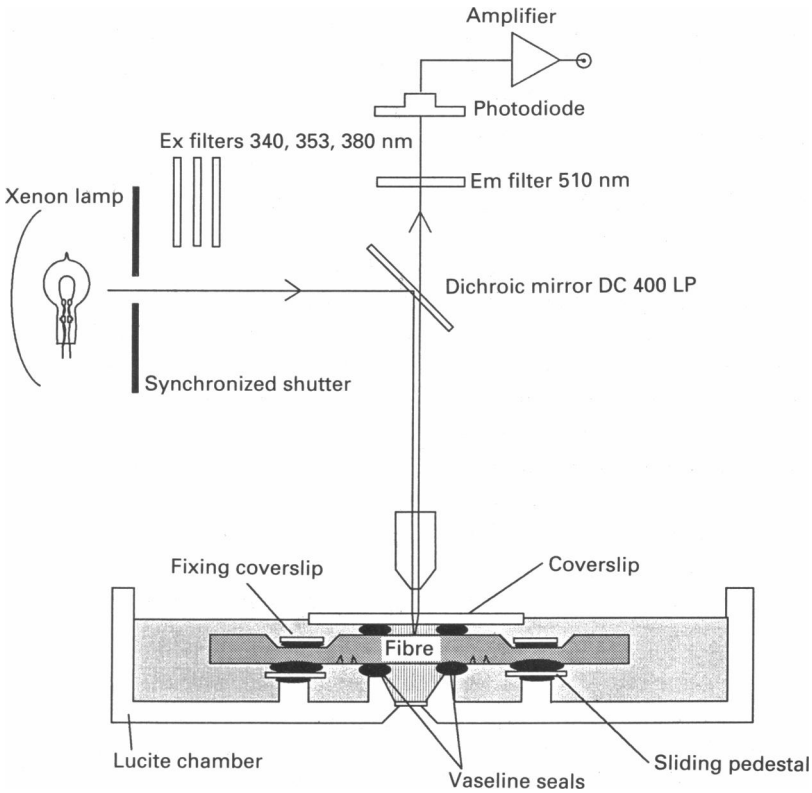

Fig. 1. Diagram of the set-up. A single extensor digitorum longus fibre was mounted in a lucite chamber. The Vaseline seals divide the recording chamber into three compartments, two lateral and one central pool. UV light was collected by a 60× air objective (Unitron, NA 0·8) after passing through the selectable interference filters (340, 353 and 380 nm) , dichroic mirror (DC 400 LP), and though an adjustable slit to reduce the size of the incident beam. Transmitted light intensities were monitored with a photodiode, after the beam was passed through the mirror and the emission filter (510 mm).

with a 75 W xenon lamp. The UV beam passed through selectable 340, 347, 353 or 380 nm excitation wavelength filters (EX filters), with 10 nm bandwidth (Omega Optical Inc., Brattleboro, VT, USA), and was reflected downward by a long-pass dichroic mirror centred at 400 nm (DC 400 LP, Omega Optical Inc.) and at a 45 deg angle. The light beam was focused onto the fibre with a 60× (NA 0·8) objective (Unitron Inc., Plainview, NY, USA), which transmitted light without major distortion up to 320 nm. After illuminating the fibre, the upward emitted light beam was collected by the objective and stimulated the photodiode (UDT-455UV, UDT Sensors Inc., Hawthorne, CA, USA) after passing through the long-pass dichroic mirror and an emission filter (EM filter) centred at 510 nm with 40 nm bandwidth. The photodiode current was recorded with a current-to-voltage converter with 1 GΩ feedback resistance to improve the signal-to-noise ratio.

The frequency response was adjusted to 5 kHz with a high frequency booster using an intermittent light source. The fibre was periodically illuminated during stimulation using a computer-controlled shutter (Uniblitz, Rochester, NY, USA). All the records were corrected for photobleaching. In resting conditions fibre illumination caused a linear decline of fluorescence with time. The mean value of $(dF_{380}/dt)/F_{380}$ was $-1{\cdot}38 \times 10^{-4} \pm 0{\cdot}18 \times 10^{-4}$ s^{-1} ($n = 10$). In most of our records the bleaching correction at 6 s after a 200 ms pulse to 0 mV represented 5% of the signal and about 0·5% of resting fluorescence.

Stimulation, recording and data analysis. An IBM compatible AT personal computer was used. Digital-to-analog and analog-to-digital conversion, 12 bits, were done by an Axolab-1 Computer interface (Axon Instruments, Inc., Foster City, CA, USA). Stimulation protocols are detailed in Results for each group of experiments. Fluorescent signals were filtered at 0·3 of the sampling frequency (−3 dB point) with a 4-pole Butterworth low-pass filter (Frequency Devices, Inc., Haverhill, MA, USA). Background autofluorescence was recorded before the addition of the dye and was subtracted from all optical records. Fluorescence signals can be normalized to basal dye fluorescence in resting conditions (without stimulation) or transformed into Ca^{2+} concentration. All the experiments were carried out at $17 \pm 0{\cdot}2$ °C. Values are given as means ± S.E.M. with the number of observations in parentheses.

In vitro calibration. The measurements were performed with Fisher spectrophotometer cells (3 ml and 1 mm light path) in a double-beam spectrofluorometer (SLM Aminco Instruments, Inc., Urbana, IL, USA) (Fig. 2*A*). Thin glass capillary cells (Vitro Dynamics; 0·1 mm path length and 2 mm width) were used to calibrate the Ca^{2+} transient recording set-up (Fig. 2*B*). The determinations in the set-up were performed at two different excitation wavelengths: at 353 nm (isosbestic point) and at 380 nm. Solutions with different Ca^{2+} concentrations were prepared following Tsien & Pozzan (1989) and using Calcium Calibration Buffer Kit II (Molecular Probes, Inc.). All the solutions contained 100 mM KCl and 10 mM Mops (3-*N*-morpholino)propanesulphonic acid) prepared in deionized water. Free Ca^{2+} levels were controlled by EGTA in the calibration solutions. The free Ca^{2+} concentrations were calculated with the following equation:

$$\text{free } Ca^{2+} = K_{D,\,EGTA} \frac{Ca^{2+}\ EGTA}{EGTA}.$$

The K_D (the dissociation constant) for mag-fura-2 was 49 μM. It is derived from the normalized fluorescence intensity − (− log Ca^{2+} concentration) plot (Fig. 2*C*). Mag-fura-5 calibration was also performed in the spectrofluorometer and in the set-up, with the same calibration solutions and analysis as those described for mag-fura-2. The K_D for mag-fura-5 in these conditions was 23 μM, very close to the value (25 μM) reported by Molecular Probes.

In vivo calibration. Intracellular Ca^{2+} concentration was calculated with the equation: $[Ca^{2+}] = K_D(R - R_{min})/(R_{max} - R)$ (Grynkiewicz, Poenie & Tsien, 1985; Klein *et al.* 1988) where K_D is the dissociation constant of the Ca^{2+}–dye reaction, $R = F_{380}/F_{353}$, R_{min} is 0% saturation of the dye by Ca^{2+} (where F_{380} and F_{353} are the fluorescence excitations at 380 and 353 nm, respectively) and R_{max} is 100% saturation (Fig. 2*B*). R_{max} was determined in the fibre with the following procedure. Fibres were isolated in the dissecting solution and placed in the recording chamber that contained the mounting solution with 10 mM glutaraldehyde grade II (Sigma Chemical Co., USA) (Delbono *et al.* 1991). After the Vaseline seals were built, the solution in the central pool was replaced by the external solution plus the same glutaraldehyde concentration, and the solution in the lateral pools by the internal solution plus 100 μM mag-fura-2. Changes in basal fluorescence (353 and 380 nm) were determined every 5 min. After 60 min, when the dye reached about 80% of the concentration in the lateral pools, the external solution was substituted with modified Krebs solution plus 1 μM ionomycin (Calbiochem, La Jolla, CA, USA) and 10 mM glutaraldehyde. With this procedure, Ca^{2+} entered into the cell in sufficient quantity without causing mechanical movement and/or disruption of the cellular architecture to saturate mag-fura-2. This resulted in a decrease of the basal fluorescence at 380 nm wavelength. The fluorescence measured at the isosbestic point was slightly reduced by the same manoeuvre. R_{max} was calculated from the minimum fluorescence values after loading the cell with Ca^{2+}. R_{max} was also determined following the procedure described by Beuckelmann & Wier (1988) using 5 μM carbonyl cyanide *m*-chlorophenylhydrazone (CCCP; Sigma) and 2 μM rotenone (Sigma) in order to avoid fibre movement by metabolic poisoning of the muscle cell. Both procedures gave consistent results for R_{max} determinations ($0{\cdot}29 \pm 0{\cdot}04$, $n = 7$).

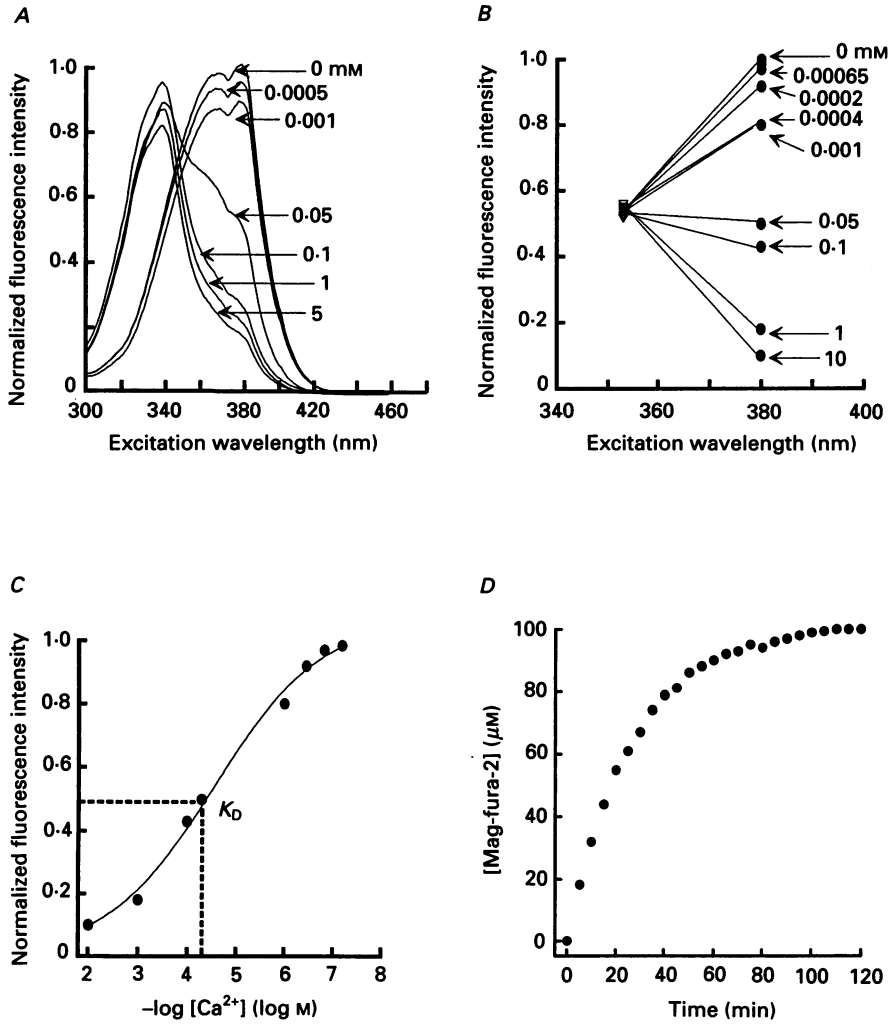

Fig. 2. Diffusion and calibration of mag-fura-2. *A*, mag-fura-2 calibration in a spectrofluorometer. Each trace corresponds to the use of different Ca^{2+} calibrating solutions (values are indicated with arrows). Temperature 22 °C. *B*, mag-fura-2 calibration in the set-up at 353 and 380 nm excitation wavelength. Here we used a more complete set of Ca^{2+} calibrating solutions than in *A*. *C*, the K_D of mag-fura-2 for Ca^{2+} (49 μM) was obtained by plotting the data from panel *B versus* $-\log[Ca^{2+}]$. *D*, at time zero the concentrations of mag-fura-2 in both lateral pools were 100 μM. Temperature 17 °C, diameter 45 μm, 3·8 μm per sarcomere, holding potential 0 mV. Determinations of fluorescence were done at 353 nm every 5 min and the dye concentration was calculated using the relationship $[\text{dye}] = IF_{353}/d^2$ (see Methods).

Attempts to measure R_{max} after permeabilizing the fibres with saponin or maximal caffeine contractures were unreliable due to the gross distortion of the fibre geometry. The R_{max} for fura-2 was obtained with long depolarizing pulses, when the dye was completely saturated with Ca^{2+}.

R_{min} was determined in the presence of the external solution and internal solution previously referred to, in the presence of 10 mM EGTA and 100 μM mag-fura-2. In these conditions, neither the replacement of the external solution with a higher Ca^{2+} concentration, nor depolarizing pulses

under voltage-clamp conditions, further reduced the basal fluorescence. This indicates the adequacy of intracellular Ca^{2+} chelation. The R_{min} value from seven determinations was $2{\cdot}68 \pm 0{\cdot}34$.

In order to determine the concentration of mag-fura-2 inside the muscle fibres, our equipment was calibrated using glass microcapillary tubes with different internal diameters (d = 100, 350 and 580 μm) and four concentrations of mag-fura-2 (10, 25, 50 and 75 μM). The measured F_{353} was plotted as a function of d^2 for each concentration of the dye using the following relationship: $[\text{dye}] = IF_{353}/d^2$, where [dye] is the dye concentration and I a calibration factor (Cantor & Schimmel, 1980; Klein *et al.* 1988).

Figure 2*D* shows the time course of mag-fura-2 entry in a fibre. The dye concentration in the fibre reached a plateau at about 90 min. This concentration was similar to the dye concentration in the lateral pools. We generally initiated Ca^{2+} transient measurements 30–40 min after mounting. At such times, the mag-fura-2 concentration inside the fibre was close to 75% of the concentration in the lateral pools. This did not affect the ratiometric $[Ca^{2+}]$ determinations since they are independent of the dye concentration.

Calculation of Ca^{2+} release. We used the model proposed by Melzer, Schneider, Simon & Szücs (1986) and Melzer, Ríos & Schneider (1987) and the mathematical formulations (appendix) by Brum, Ríos & Schneider in Brum, Ríos & Stefani (1988). This method obtained the rate of Ca^{2+} release from (dCa^{2+}/dt) = input − output flux. The input flux corresponds to the Ca^{2+} release, while the output flux to the activity of the removal system. On the assumption that the release process terminates shortly after the end of the stimulating pulse, the removal function can be obtained by fitting the decaying phase of the Ca^{2+} transient to the following differential equation:

$$d[Ca^{2+}]/dt = -(d[CaTN]/dt) - (d[CaParv]/dt) - (MF^2) - (d[CaP]/dt) - (d[CaD]/dt) - (d[CaEGTA]/dt) + L),$$

where TN is troponin; Parv, parvalbumin; M, maximum sarcoplasmic reticulum (SR) Ca^{2+} pump rate; F, fractional occupancy of pump sites (P); D, dye concentration and L the Ca^{2+} leak from the SR. Parv equilibrates with [CaParv] and [MgParv] and MF^2 corresponds to $M([CaP]/[P_t])^2$ where P_t is the total concentration of pump sites. The parameters were: [TN], $k_{on,CaTN}$, $k_{off,CaTN}$, [Parv], $k_{on,CaParv}$, $[Mg^{2+}]$, $k_{on,MgParv}$, $k_{off,MgParv}$, M, P_t, [dye], $k_{on,Cadye}$, $k_{off,Cadye}$, [EGTA], $k_{on,CaEGTA}$, and $k_{off,CaEGTA}$, where k_{on} and k_{off} are the rate constants for association and dissociation of calcium or magnesium from the myoplasmic calcium binding protein, calcium pump and external buffers. The following nine parameters were fitted: [TN], $k_{on,CaTN}$, $k_{off,CaTN}$, [Parv], $k_{on,CaParv}$, $k_{on,MgParv}$, $k_{off,MgParv}$, M and P_t with boundaries close to the corresponding biochemical determinations. Euler's method was used to solve the differential equations and a least-square fit for the decaying phase of the Ca^{2+} transient 14 ms after fibre repolarization.

RESULTS

Ca^{2+} transients in current clamp conditions

Action potentials were elicited in modified Krebs solution and with K^+ as the main intracellular cation. Figure 3 shows action potentials (continuous line) and Ca^{2+} transients (dotted lines) detected with 400 μM mag-fura-2 (*A*) and 50 μM fura-2 (*B*). The peak $[Ca^{2+}]$ was $4{\cdot}6 \pm 0{\cdot}4$ μM in mag-fura-2. The following parameters were measured from the Ca^{2+} transients elicited by the action potentials: time to peak ($4{\cdot}6 \pm 0{\cdot}42$ ms), half-width ($8{\cdot}2 \pm 1{\cdot}5$ ms), time constant of the rising phase ($1{\cdot}15 \pm 0{\cdot}25$ ms), time constant of the decaying phase ($3{\cdot}26 \pm 0{\cdot}65$ ms), delay between the initiation of action potential and Ca^{2+} transient ($2{\cdot}0 \pm 0{\cdot}2$ ms) (n = 5). In order to compare the time course of the Ca^{2+} transients using dyes with low (mag-fura-2) and high affinity for Ca^{2+}, a Ca^{2+} transient recorded with fura-2 is illustrated in panel *B*. Since the fura-2 signal is saturated at the peak of the transient (100% Ca^{2+}-fura-2 complex), the Ca^{2+} signal was measured as a percentage of dye saturation instead of Ca^{2+} concentration. Fura-2 signal is slower than with mag-fura-2. The time to peak in fura-2 (n = 5) was $9{\cdot}4 \pm 1{\cdot}5$ ms, the half-width 120 ± 17 ms, the time constant of

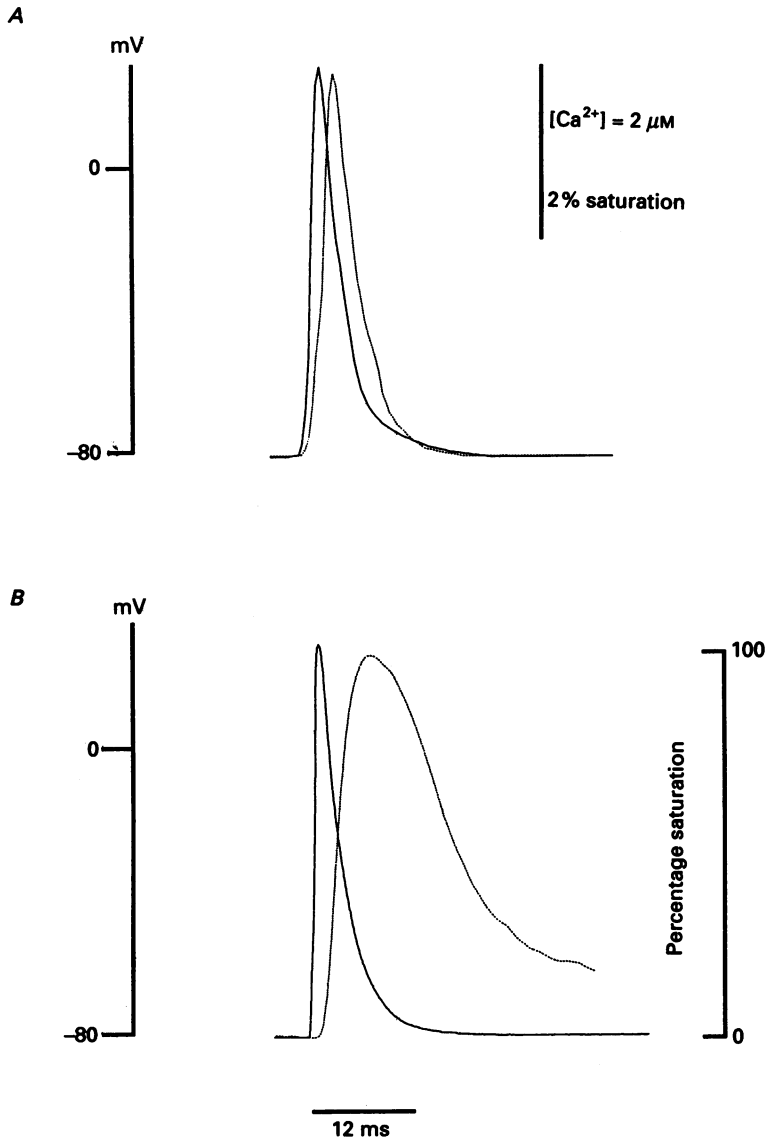

Fig. 3. Ca^{2+} transients elicited by action potentials. Action potentials (continuous line) in modified Krebs solution were detected with 400 μM mag-fura-2 (*A*) and 50 μM fura-2 (*B*) (dotted line) with pulses from −80 mV. Temperature 17 °C, 3·6 μm per sarcomere. Voltage scale is presented at the left of the traces. The mag-fura-2 Ca^{2+} transient (*A*) is expressed in Ca^{2+} concentration while the fura-2 transient is expressed as percentage saturation of the dye.

the rising phase $13{\cdot}8 \pm 1{\cdot}8$ ms, the time constant of the decaying phase $76{\cdot}9 \pm 8{\cdot}7$ ms and the delay between the initiation of action potential and Ca^{2+} transient $3{\cdot}8 \pm 0{\cdot}3$ ms ($n = 5$). These differences in the time course of the Ca^{2+} transient can be attributed to the lower affinity of mag-fura-2 with a faster off rate (see Discussion).

Ca^{2+} transients and Ca^{2+} release in voltage clamp

In order to study the process of Ca^{2+} release at different pulse voltages and durations, Ca^{2+} transients were recorded under voltage-clamp conditions. Figure 4*A* shows Ca^{2+} transients obtained by applying 75 ms depolarizing pulses from -50 to 20 mV in 10 mV increments (holding potential of -80 mV) (*B*). The first pulse to -50 mV (first trace from the bottom) did not indicate any increase in Ca^{2+} concentration. This can be explained by the relatively low mag-fura-2 affinity for Ca^{2+} since under equivalent experimental conditions with the high-affinity Ca^{2+} dye, fura-2, Ca^{2+} transients could be detected at -55 mV. Ca^{2+} transients at -40 mV (second trace from the bottom) reached a plateau, which slightly decreased during the pulse. After repolarization the signal quickly returned to the level recorded prior to pulse application. The subsequent Ca^{2+} transient at -30 mV shows two phases, an initial fast peak (T_1) followed by a second slow rise in Ca^{2+} concentration, leading to a second larger peak (T_2). The amplitude of the Ca^{2+} transient increased as more depolarizing pulses were applied. The rising phase became faster, and the decaying phase became progressively slower. The peak Ca^{2+} value from twenty-two fibres (from different muscles) was $10{\cdot}5 \pm 1{\cdot}3$ μM. The Ca^{2+} concentration–membrane potential relationship was plotted in panel *C* for isochronal determinations (T_1 at 5 and T_2 at 70 ms) of both Ca^{2+} transients components. The experimental points were fitted to a Boltzmann function of the form $[Ca^{2+}]_V = [Ca^{2+}]_{max}/(1+\exp((V_{\frac{1}{2}}-V)/K))$, where $[Ca^{2+}]_V$ is the Ca^{2+} concentration at different voltages V, $[Ca^{2+}]_{max}$ is the maximum Ca^{2+} concentration, $V_{\frac{1}{2}}$ is the mid-point potential of the curve, and K the slope factor. Values for T_1 and T_2 were: $[Ca^{2+}]_{max}$ 8·1 and 14·7 μM, $V_{\frac{1}{2}}$ $-12{\cdot}1$ and $-15{\cdot}5$ mV and K 13·5 and 10·2 mV, respectively. Superimposed on the decaying phase of the Ca^{2+} transients are shown the best fittings (see below).

Since the Ca^{2+} transient is a very complex signal resulting from the release process together with the various Ca^{2+} buffering and Ca^{2+} uptake systems, a better evaluation on the role of the membrane potential on the Ca^{2+} release process can be obtained by calculating the Ca^{2+} rate of release. For this purpose, we assume that Ca^{2+} release is negligible shortly after the termination of the pulse (14 ms) and that Ca^{2+} decay after the pulse reflects the activity of the various components of the Ca^{2+} removal process. This assumption seems reasonable since in our experimental conditions Ca^{2+} transients decay with a single exponential time course for different pulse durations (see below). Another assumption is that the same rates of removal obtained from the decay of the Ca^{2+} transient after the pulse, also apply to the Ca^{2+} transient during the depolarizing pulse. Figure 5 shows Ca^{2+} release records (dCa^{2+}_{REL}/dt function or R_{REL} in Melzer *et al.* (1987)) (*A*) obtained from fitting the removal function to the decay phase of the Ca^{2+} transient (see Methods) (*B*) and the voltage dependence of the Ca^{2+} release process (*C*). The record in *B* exemplifies an isolated Ca^{2+} transient record at $+10$ mV and the superimposed fitted trace to the decay phase. The values that better fitted the Ca^{2+} transient decaying phase (fitting

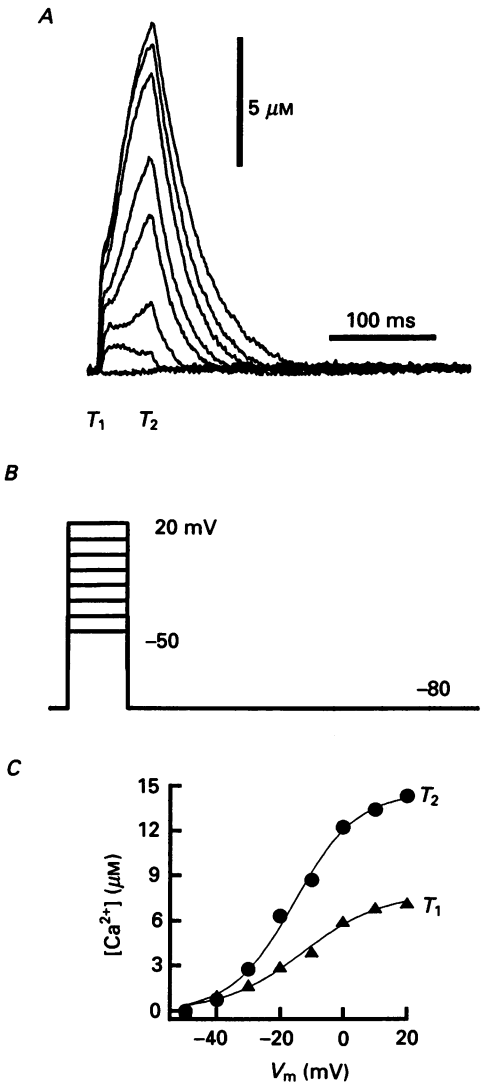

Fig. 4 . Ca^{2+} transients in voltage-clamped fibres. Mag-fura-2 signals at different voltages. Ca^{2+} transients during depolarizing pulses of 75 ms duration from −80 mV (holding potential) to +20 mV with 10 mV increments. Fitting traces to the decaying phase of the Ca^{2+} transients are superimposed (*A*). The traces correspond (from bottom to top) to −50 to +20 mV (*B*). Pulses more positive than −40 mV gave rise to two phases (T_1 and T_2) in the Ca^{2+} transient. The isochronic determinations of the Ca^{2+} transients were plotted in *C*. Both sets of data were fitted to a Boltzmann function. V_m, membrane potential.

traces superimposed in Fig. 4) were: $k_{off,MgParv} = 6{\cdot}5\ s^{-1}$, $M = 2000\ \mu M^{-1}\ s^{-1}$, [Parv] = 430 μM, $k_{off,CaParv} = 1{\cdot}0\ s^{-1}$, $k_{off,CaTN} = 600\ s^{-1}$, $K_D = 1{\cdot}0\ \mu M$, $P_t = 1{\cdot}0\ \mu M$, $k_{on,MgParv} = 0{\cdot}06\ \mu M^{-1}\ s^{-1}$, $k_{on,CaParv} = 100\ \mu M^{-1}\ s^{-1}$, $[Mg^{2+}]_{rest} = 1000\ \mu M$, $k_{on,CaTN} = 85\ \mu M^{-1}\ s^{-1}$, [TN] = 240·0 μM, $[Ca^{2+}]_{rest} = 0{\cdot}05\ \mu M$.

The derived rate of release (Fig. 5*A*) at −40 mV showed first a rapid component

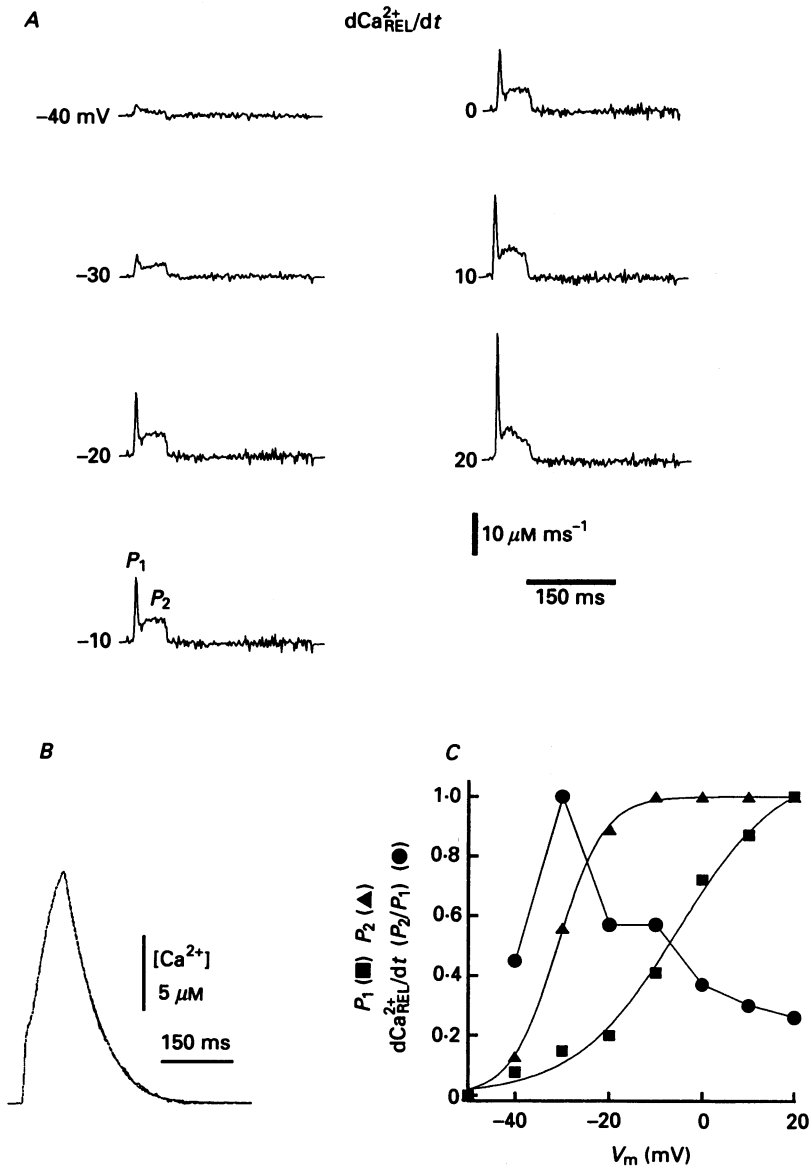

Fig. 5. Rate of Ca^{2+} release. *A*, rate of Ca^{2+} release corresponding to the Ca^{2+} transients shown in Fig. 4. At −40 mV, there is just one component of the rate of release, and a steady state is reached until the end of the pulse. From −30 mV onward, a second component becomes evident. At +10 mV, the rate of Ca^{2+} release was $17{\cdot}2 \pm 3{\cdot}1$ μM ms^{-1} ($n = 10$). *B*, the Ca^{2+} transient at +10 mV and the fitting trace to the decaying phase 14 ms after cutting the pulse are superimposed, in order to calculate dCa^{2+}_{REL}/dt. Temperature 17 °C, 3·7 μm per sarcomere. *C*, the voltage dependence of the first (P_1, ■), and second component (P_2, ▲) of the rate of release from panel *A*. The points were fitted to a Boltzmann function. The rate of release ratio between P_2 and P_1 is also represented (●).

(P_1), and then a plateau (P_2) similar to the Ca^{2+} release in the frog (Melzer *et al.* 1986). From −30 mV to more positive potentials, a second Ca^{2+} release increment, which was separated from the first spike release component, became evident. For pulses at +20 mV and 100 ms duration, the peak rate of Ca^{2+} release was $17{\cdot}2 \pm 3{\cdot}1$ μM ms^{-1} ($n = 10$).

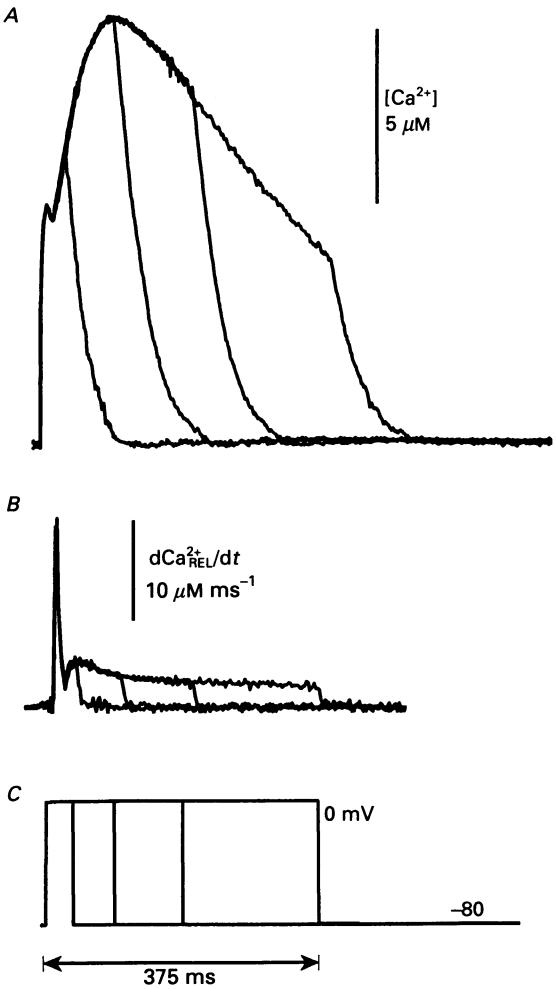

Fig. 6. Ca^{2+} transients and Ca^{2+} rate of release with different pulse duration. *A*, Ca^{2+} transients with different pulse duration. Fitting traces to the decaying phase of the Ca^{2+} transients are superimposed. *B*, the rate of Ca^{2+} release shows an initial fast component and a second phase that declines till the end of the pulse. *C*, pulses of 62, 125, 250 and 375 ms duration from holding potential of −80 mV to 0 mV. The highest rate of release reached was 21 μM ms^{-1}. 3·7 μm per sarcomere.

Figure 5*C* shows the voltage dependence of the peak release P_1 (■), the second peak release P_2 (▲) and the P_2/P_1 ratio (●). P_1 became noticeable at −40 mV and increased progressively to 20 mV with a slope factor of 11 mV. The second component P_2 was also detected at −40 mV, but it rapidly reached saturation at

-10 mV (slope, 11 mV). The $V_{\frac{1}{2}}$ values from the fitting with a Boltzmann function were $-5{\cdot}3$ and -30 mV, respectively. The P_2/P_1 ratio shows a peak at -30 mV that coincides with the appearance of the rising phase in the second component. With further depolarizations, the relative weight of the first component P_1 progressively increased.

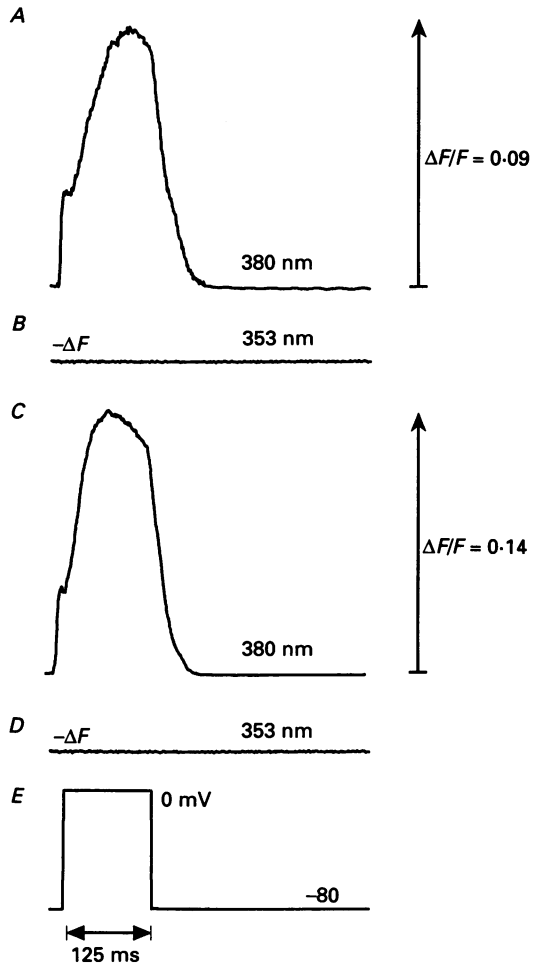

Fig. 7. Comparison of Ca^{2+} transients studied with mag-fura-5 and mag-fura-2. Panels *A* and *B* show the fluorescence signals obtained with mag-fura-5 (K_D for $Ca^{2+} = 23$ μM) at 380 and 353 nm excitation, respectively. Panels *C* and *D* show the same type of signals obtained with mag-fura-2 (K_D for $Ca^{2+} = 49$ μM) in another fibre. The pulse protocol is depicted in panel *E*. Fluorescence signals were normalized per basal fluorescence.

Ca^{2+} transients and Ca^{2+} release with different pulse duration

Ca^{2+} transients with different pulse durations and a 2 min stimulating interval are shown in Fig. 6*A*. The fitting to the decaying phase of the Ca^{2+} transients are superimposed. Pulses of 62, 125, 250 and 375 ms duration from a holding potential of -80 to 0 mV are shown in panel *C*. As previously shown, Ca^{2+} transient records

had two phases, an initial fast component followed by a second component, which increased more slowly than the first one and decayed during the pulse. After the pulses were cut off, Ca^{2+} transient records decayed exponentially to the basal Ca^{2+} concentration recorded prior to the application of the pulses. The rate of Ca^{2+} release (panel *B*) showed an initial fast component and the second phase. After the sharp initial phase there was a second upward component that declined smoothly until the end of the pulse. The peak rate of release reached 21 μM ms^{-1}.

Comparison of Ca^{2+} transients studied with mag-fura-2 and mag-fura-5

Figures 4–6 show, as a predominant characteristic of mammalian Ca^{2+} transients, the presence of a second slow rising phase. These measurements were planned to evaluate the possible participation of mechanical artifacts and/or a Mg^{2+} signal in the generation of the complex time course of the Ca^{2+} transient. To this end we measured fluorescence signals at the dye isosbestic point (353 nm), and we used mag-fura-5 which is more sensitive to changes in myoplasmic Mg^{2+} concentration. Figure 7*A* and *B* shows fluorescent signals obtained with mag-fura-5 (K_D for Ca^{2+} = 23 μM and for Mg^{2+} = 0·5 mM, see Methods) at 380 and 353 nm excitation wavelength, respectively. Panel *C* and *D* show equivalent signals from another fibre obtained with mag-fura-2 (K_D for Ca^{2+} = 49 μM and for Mg^{2+} = 5 mM). The pulse protocol is depicted in panel *E*. The records at 353 nm show no detectable signal at the same gain. This confirms the isosbestic point for both dyes and rules out the participation of a mechanical artifact in the 'hump' of the rising phase of mag-fura-2 and mag-fura-5 signals. Furthermore, mag-fura-2 and mag-fura-5 signals are practically indistinguishable in their time courses. Since mag-fura-5 has a higher affinity for Mg^{2+}, we used this ability to explore more accurately a potential Mg^{2+} transient interference in our Ca^{2+} transients monitored with mag-fura-2. The K_D ratio for Ca^{2+} between both dyes (mag-fura-2/mag-fura-5) is about 2 (49/23 μM), while the K_D ratio for Mg^{2+} is 10 (5/0·5 μM). In summary, these observations suggest that mechanical artifacts and/or changes in intracellular Mg^{2+} cannot explain the complex time course of the fluorescence signals and calculated Ca^{2+} transients.

Effect of voltage on the decaying phase of free myoplasmic Ca^{2+} concentration after repolarization

Figure 8*A* shows the decaying phase of Ca^{2+} transients records shown in Fig. 4*A*. Each trace was fitted with an exponential function plus a constant. The fitting started 14 ms after cutting the pulse. Fitting curves are superimposed to each experimental trace. Panel *B* shows the decay time constant–membrane potential relationship. A progressive increase can be seen in the decay time constant of the transients with increments in pulse amplitude. A saturation trend with larger pulses can be observed. The time constant of decay is highly dependent on the elapsed time between pulses; in these experiments we used a 2 min interval between pulses, a time that was considered long enough to return myoplasmic Ca^{2+} concentration to resting values (Klein, Kovács, Simon & Schneider, 1991).

Effect of pulse duration on the decaying phase of free myoplasmic Ca^{2+} after repolarization

Figure 8*C* shows the decaying phase of Ca^{2+} transients elicited by different pulse durations with the same analysis as in Fig. 8*A*. The decay phase was fitted to a single

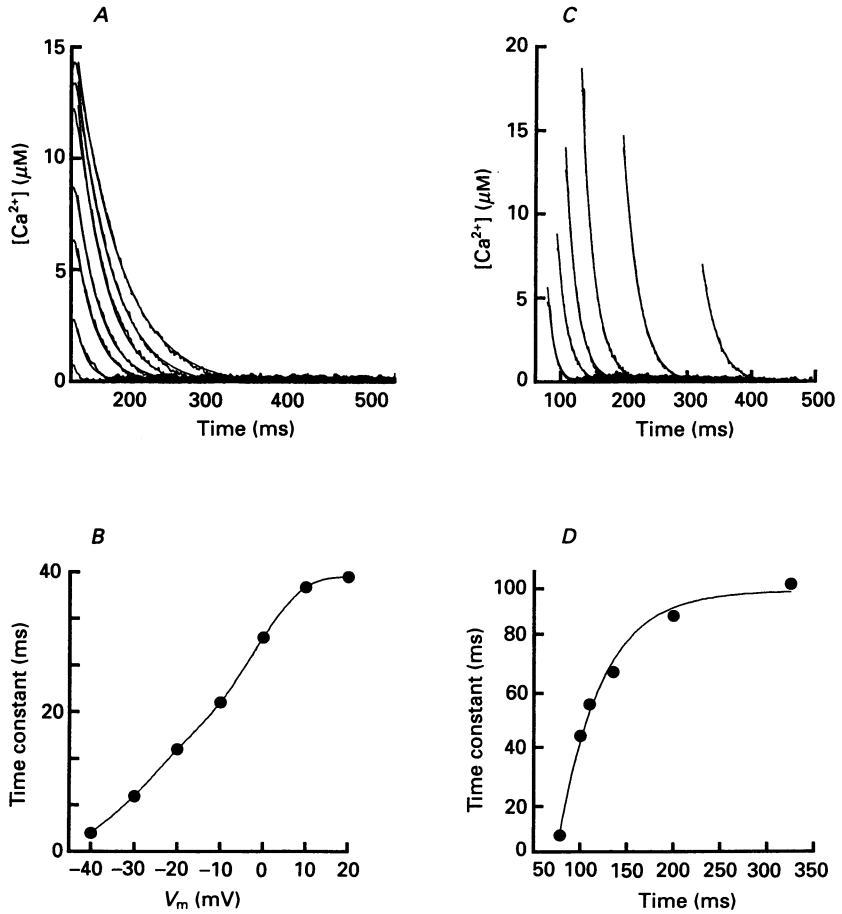

Fig. 8. Effect of voltage and pulse duration on the decaying phase of free myoplasmic Ca^{2+} after repolarization. Panel *A* shows the decaying phase of the Ca^{2+} transients shown in Fig. 4*A*. Each trace was fitted with an exponential function plus a constant ($a \times \exp(-x/t)+b$), where b is a constant. *B*, time constant of the decaying phase of the Ca^{2+} transients *vs.* V_m relationship. Same fibre as in Fig. 5, 3·8 μm per sarcomere. *C*, decaying phase of Ca^{2+} transients elicited by different pulse durations. Each trace was fitted and plotted in *D* as the Ca^{2+} transient decaying phase *vs.* time relationship. 3·7 μm per sarcomere.

exponential, whose time constant progressively increased with pulse duration. Panel *D* shows the pulse duration dependence of the time constant of decay. As for pulses of increasing amplitudes (Fig. 8*A*), the decay of the Ca^{2+} transient time constant increased with pulse duration reaching a limiting value for pulses larger than 200 ms.

DISCUSSION

Myoplasmic Ca^{2+} concentration in mammalian skeletal muscle can be accurately monitored with the fluorescent dye mag-fura-2 with negligible delay, in fibres at 3·6–3·8 μm sarcomere length. The use of mag-fura-2 instead of AP III gives some advantages: (i) Ca^{2+}: dye stoichiometry during the Ca^{2+} release process does not change, (ii) there is a very short lag in the appearance of the dye signal in the centre of the fibre, and (iii) very fast response of the dye to modifications of myoplasmic Ca^{2+} concentrations. These features enabled us to study the biphasic rising phase of the Ca^{2+} transient and the fast decay of this signal after interrupting the stimulation. We found that the amount of Ca^{2+} detected during an action potential and under voltage-clamp conditions was similar to that in frog muscle. The released Ca^{2+} under voltage clamp was higher than in cut frog fibres but lower than in intact frog fibres (see below).

Calcium transient studied with mag-fura-2

The time course of the Ca^{2+} transients in this work shows some similarities with the signals obtained with AP III in frog and mammalian skeletal muscle fibres. Ca^{2+} transients studied with AP III in frog muscle show two distinct rising phases: an early rapid rise and a slower later phase separated by a decay or a plateau (Brum *et al.* 1988). With AP III and mag-fura-2, the maximum Ca^{2+} concentration is usually reached during the second component (Brum *et al.* 1988). The average Ca^{2+} transient in frog muscle determined with AP III with pulses between 230 and 750 ms was $12{\cdot}1 \pm 3{\cdot}5$ μM (Brum *et al.* 1988). This value is similar to that obtained in this work ($10{\cdot}5 \pm 1{\cdot}3$ μM, $n = 22$). The average peak amplitude of Ca^{2+} concentration detected with mag-fura-2 in frog fibres elicited with action potentials was 5 μM (Konishi *et al.* 1991) but it is in disagreement with determinations with other dyes such as PDAA (10 μM; Konishi & Baylor, 1991) and AP III (2 μM). The binding of these dyes to myoplasmic constituents is the inverse to the peak Ca^{2+} values determined (75, 42–51 and 22–44 % respectively; Konishi *et al.* 1991). If nearly 50 % of mag-fura-2 is bound to myoplasmic constituents, the calculation of the change in Ca^{2+} concentration from the value $\Delta F/F$ would be underestimated by a factor of 2. Therefore, the actual concentration obtained with mag-fura-2 would be twice the value obtained in this work. The AP III binding to intracellular components would also influence the Ca^{2+} concentration determinations, and could at least partially explain differences in the peak Ca^{2+} concentration obtained previously in rat muscle fibres (García & Schneider, 1992). The differences in sarcomere length can also explain the higher peak Ca^{2+} concentrations obtained in our voltage-clamp experiments compared with García & Schneider's communication (1992).

In this work, Ca^{2+} transients in response to action potentials show very similar kinetics to the records obtained with mag-fura-2 and AP III in frog muscle (Konishi *et al.* 1991). The very fast fluorescence response to voltage pulses allows us to monitor changes in myoplasmic Ca^{2+} concentrations with little or no kinetic delay. This delay with mag-fura-2 has been estimated to be 0·2 ms (Konishi *et al.* 1991).

From our work, we conclude that after interrupting the pulse, the myoplasmic calcium concentration stopped rising and slowly decayed to levels close to those

before stimulation. The decaying phase of the Ca^{2+} transients with different voltage and pulse durations is a parameter that we can analyse to indicate that only the removal process operates after repolarization (Melzer *et al.* 1986).

Complex time course of the Ca^{2+} transient

Ca^{2+} release and the resulting Ca^{2+} transients in mammalian fibres have a prominently slow second phase with a rising component that occurs after the initial fast release peak. One explanation for this phenomenon is that an amplified release process together with a highly non-linear removal system produces a highly non-linear change in the shape of the Ca^{2+} transient, giving rise to the appearance of a second rising phase (see Fig. 13 of Brum *et al.* 1988). A second explanation of the 'hump' in the rising phase of the Ca^{2+} transient is that it is a mechanical artifact. However, it is not likely because the mechanical artifact occurs in an opposite direction to the Ca^{2+} transient (see Methods). Furthermore, the 'hump' remained unchanged when we improved the signal-to-noise ratio by increasing the mag-fura-2 concentration to 400 μM. A third explanation is that a Mg^{2+} transient would be detected by mag-fura-2. From data observed in frog muscle after a 100–200 ms pulse, the Mg^{2+} concentration is in the range of 47–70 μM (Baylor, Quinta-Ferreira & Hui, 1985; Irving, Maylie, Sizto & Chandler, 1989). To clarify this point, we used mag-fura-5, which has 10 times more affinity for Mg^{2+} and only twice the affinity for Ca^{2+} than mag-fura-2. If the 'hump' were a consequence of a Mg^{2+} transient, we should be able to detect this break in the rising phase more accurately with mag-fura-5. As seen in Fig. 7, there is no significant difference between the two dyes. On the other hand, experiments performed with AP III in frog fibres in current and voltage clamp, at 3·7 μm sarcomere length, and at 18 °C, the Mg^{2+} transients have an early start. However, multiple components in the rising phase of the Ca^{2+} transients in these records cannot be detected (Irving *et al.* 1989). In summary, although we cannot rule out a highly non-linear removal system, it is unlikely that the second rising phase is a consequence of a mechanical artifact or a Mg^{2+} transient.

Rate of Ca^{2+} release from the sarcoplasmic reticulum

The model we used to analyse the calcium removal system (Robertson, Johnson & Potter, 1981; Melzer, Ríos & Schneider, 1986; Simon & Schneider, 1988) takes into consideration the decaying of Ca^{2+} concentration, beginning 14 ms after fibre repolarization. It is assumed that SR Ca^{2+} release is almost completely turned off during that period, and the rapid decline in Ca^{2+} concentration seen during a Ca^{2+} transient record is an indication of a brisk termination of Ca^{2+} release after fibre repolarization. This model also assumes a spatially uniform change in myoplasmic Ca^{2+} concentration after fibre depolarization (but see Cannell & Allen, 1984). Furthermore, it is also assumed that there is neither fibre run-down nor dye modification of the Ca^{2+} binding and transport ability of intracellular Ca^{2+} binding proteins (Melzer *et al.* 1986). Thus, using this model, we obtain dCa^{2+}_{REM}/dt (rate of Ca^{2+} removal) by adding dCa^{2+}_{F}/dt (rate of Ca^{2+} bound to rapidly equilibrating myoplasmic buffers such as troponin and Ca^{2+} dye) and dCa^{2+}_{REL}/dt (Melzer *et al.* 1987). Our initial conditions for the fitting routine (see Methods for free parameters used in the fit) are obtained mainly from mammalian twitch skeletal muscle because

the best fitted parameters obtained from the frog (Brum *et al.* 1988) do not accurately describe the Ca^{2+} removal process from the myoplasm in rat EDL fibres. When data for the fitting were not available, information from frog fast muscle was used. Therefore, in this work, $K_{D,TN} = 7{\cdot}1$ μM ($k_{off,CaTN} = 600$ s^{-1}; $k_{on,CaTN} = 85$ μM^{-1} s^{-1}) differs from the value reported by Brum *et al.* (1988) (9·6 μM). This $K_{D,TN}$ for Ca^{2+} in mammalian muscle is higher than in amphibian, where the value is 3·13 μM (k_{off} = 300 s^{-1}; $k_{on} = 1 \times 10^8$ M^{-1} s^{-1}) (Potter, Johnson, Dedman, Schreiber, Mandel, Jackson & Means, 1977).

The $K_{D,Parv}$ obtained in this work is 0·01 μM ($k_{off} = 1$ s^{-1}; $k_{on} = 100$ M^{-1} s^{-1}). This value is about half of that reported by Brum *et al.* (1988) (0·0196 μM), and differs from those determined by Blum, Lehky, Kohler, Stein & Fisher (1977) in rabbit, and Heizmann, Malencik & Fisher (1974) in chicken (see Heizmann, 1984; Hou, Johnson & Rall, 1991).

The K_D for Ca^{2+} of the sarcoplasmic reticulum Ca^{2+} pump in this work (1 μM) does not differ significantly from the value calculated in amphibian muscle fibres (Brum *et al.* 1988). The maximum pump rate (2000 μM s^{-1}) in our mammalian preparation differs from the amphibian (pump V_{max}, 2824 μM s^{-1}; Klein *et al.* 1991).

The rate of Ca^{2+} release calculated in this work (17·2 $\pm$ 3·1 μM ms^{-1}) is higher than the rate obtained in cut frog and mammalian fibres (Melzer *et al.* 1987; García & Stefani, 1990). In intact frog fibres, the total $d[Ca]_T/dt$ was 38 μM ms^{-1} (Baylor, Chandler & Marshall, 1983) with arzenazo III, and about 98 μM ms^{-1} (Baylor & Hollingworth, 1988) with AP III. Most of the experiments with frog muscle are carried out at 7–10 °C and consequently lower rates of Ca^{2+} release are calculated. It should be pointed out that the latter two works by Baylor *et al.* were performed at 16–17 °C. This temperature accelerates the Ca^{2+} release process.

This study was supported by a National Institutes of Health (USA) grant R01-AR38970, by grants from the Muscular Dystrophy Association to E.S. and MDA fellowship to O.D. We are grateful to Ariel Escobar for participating in the initial *in vitro* dye calibrations and helpful discussion during the developing of this project, to William P. Schilling for discussions about dye calibrations, to Eduardo Ríos who kindly gave us an updated version of the fitting program, and to Alice Chu for her helpful discussion of the manuscript.

REFERENCES

BAYLOR, S. M., CHANDLER, W. K. & MARSHALL, M. W. (1983). Sarcoplasmic reticulum calcium release in frog skeletal muscle estimated from Arzenazo III calcium transients. *Journal of Physiology* **344**, 625–666.

BAYLOR, S. M. & HOLLINGWORTH, S. (1988). Fura-2 calcium transients in frog skeletal muscle fibres. *Journal of Physiology* **403**, 151–192.

BAYLOR, S. M., QUINTA-FERREIRA, M. E. & HUI, C. S. (1985). Isotropic components of Antipyrylazo III signals from frog skeletal muscle fibers. In *Calcium in Biological Systems*, ed. RUBIN, R. P., WEISS, G. & PUTNEY, J. W. JR, pp. 339–349. Plenum Press, New York.

BEUCKELMANN, D. J. & WIER, W. G. (1988). Mechanism of release of calcium from sarcoplasmic reticulum of guinea-pig cardiac cells. *Journal of Physiology* **405**, 233–255.

BLUM, H. E., LEHKY, P., KOHLER, L., STEIN, E. A. & FISCHER, E. H. (1977). Comparative properties of vertebrate parvalbumin. *Journal of Biological Chemistry* **252**, 2834–2838.

BRUM, G., RÍOS, E. & STEFANI, E. (1988). Effect of extracellular calcium movements of excitation–contraction coupling in frog skeletal muscle fibres. *Journal of Physiology* **398**, 441–473.

CANNELL, M. B. & ALLEN, D. G. (1984). Model of calcium movements during activation in the sarcomere of frog skeletal muscle. *Biophysical Journal* **45**, 913–925.

CANTOR, C. R. & SCHIMMEL, P. R. (1980). *Biophysical Chemistry*, part II, *Techniques for the Study of Biological Structure and Function*, pp. 439. W. H. Freeman and Company, San Francisco.

DELBONO, O. (1992). Calcium current activation and charge movement in denervated mammalian skeletal muscle fibres. *Journal of Physiology* **451**, 187–203.

DELBONO, O., GARCÍA, J., APPEL, S. H. & STEFANI, E. (1991). Calcium current and charge movement of mammalian muscle: action of amyotrophic lateral sclerosis immunoglobulins. *Journal of Physiology* **444**, 723–742.

DELBONO, O. & STEFANI, E. (1992). Calcium transients in mammalian skeletal muscle fibres. *Biophysical Journal* **61**, A160.

EUSEBI, F., MILEDI, R. & TAKAHASHI, T. (1980). Calcium transients in mammalian muscles. *Nature* **284**, 560–561.

EUSEBI, F., MILEDI, R. & TAKAHASHI, T. (1985). Aequorin–calcium transients in mammalian fast and slow muscle fibers. *Biochemical Research* **6** (3), 129–138.

FABIATO, A. (1988). Computer programs for calculating total from specified free or free from specified total ionic concentrations in aqueous solutions containing multiple metals and ligands. In *Methods in Enzymology, Biomembranes*, vol. **157** part A, ed. FLEISHER, S. & FLEISHER, B., pp. 378–417. Academic Press, Inc., San Diego, CA, USA.

FRANCINI, F. & STEFANI, E. (1989). Decay of the slow calcium current in twitch muscle fibers of the frog is influenced by intracellular EGTA. *Journal of General Physiology* **94**, 953–969.

GARCÍA, J. & SCHNEIDER, M. F. (1992). Modulation of calcium transients and calcium release in rat skeletal muscle fibers. *Biophysical Journal* **61**, A25.

GARCÍA, J. & STEFANI, E. (1990). Calcium transients in rat skeletal muscle: evidence for a Ca^{2+}-regulated Ca^{2+} release process. *Biophysical Journal* **57**, 400a.

GRYNKIEWICZ, G., POENIE, M. & TSIEN, R. Y. (1985). A new generation of Ca^{2+} indicators with greatly improved fluorescent properties. *Journal of Biological Chemistry* **260**, 3440–3450.

HEIZMANN, C. W. (1984). Parvalbumin, an intracellular calcium-binding protein; distribution, properties and possible roles in mammalian cells. *Experientia* **40**, 910–921.

HEIZMANN, C. W., MALENCIK, D. A. & FISCHER, E. H. (1974). Generation of parvalbumin-like proteins from troponin. *Biochemical and Biophysical Research Communications* **57**, 162–168.

HIROTA, A., CHANDLER, W. K., SOUTHWICK, P. L. & WAGGONER, A. S. (1989). Calcium signals recorded from two new purpurate indicators inside frog cut twitch fibers. *Journal of General Physiology* **94**, 597–631.

HOU, T., JOHNSON, J. D. & RALL, J. A. (1991). Parvalbumin content and Ca^{2+} and Mg^{2+} dissociation rates correlated with changes in relaxation rate of frog muscle fibres. *Journal of Physiology* **441**, 285–304.

IRVING, M., MAYLIE, J., SIZTO, N. L. & CHANDLER, W. K. (1989). Simultaneous monitoring of changes in magnesium concentrations in frog cut twitch fibers containing antipyrylazo III. *Journal of General Physiology* **93**, 585–608.

KLEIN, M. G., KOVÁCS, L., SIMON, B. J. & SCHNEIDER, M. F. (1991). Decline of myoplasmic Ca^{2+}, recovery of calcium release and sarcoplasmic Ca^{2+} pump properties in frog skeletal muscle. *Journal of Physiology* **441**, 639–671.

KLEIN, M. G., SIMON, B. J., SZÜCS, G. & SCHNEIDER, M. F. (1988). Simultaneous recording of calcium transients in skeletal muscle using high- and low-affinity calcium indicators. *Biophysical Journal* **53**, 971–988.

KONISHI, M. & BAYLOR, S. M. (1991). Myoplasmic calcium transients monitored with purpurate indicator dyes injected into intact frog skeletal muscle fibers. *Journal of General Physiology* **97**, 245–270.

KONISHI, M., HOLLINGWORTH, S., HARKINS, A. B. & BAYLOR, S. M. (1991). Myoplasmic calcium transients in intact frog skeletal muscle fibers monitored with the fluorescent indicator furaptra. *Journal of General Physiology* **97**, 271–301.

KOVÁCS, L., RÍOS, E. & SCHNEIDER, M. F. (1979). Calcium transients and intramembrane charge movement in skeletal muscle fibres. *Nature* **279**, 391–396.

KOVÁCS, L., RÍOS, E. & SCHNEIDER, M. F. (1983). Measurements and modification of free calcium transients in frog skeletal muscle fibers by a metallochromic indicator dye. *Journal of General Physiology* **343**, 161–196.

LAMB, G. D. & STEPHENSON, D. G. (1991). Calcium release in skinned muscle fibres of the toad by transverse tubular depolarization or by direct stimulation. *Journal of Physiology* **423**, 519–542.

MELZER, W., RÍOS, R. & SCHNEIDER, M. F. (1986). The removal of myoplasmic free calcium following calcium release in frog skeletal muscle. *Journal of Physiology* **372**, 261–292.

MELZER, W., RÍOS, E. & SCHNEIDER, M. F. (1987). A general procedure for determining the rate of calcium release from the sarcoplasmic reticulum in skeletal muscle fibers. *Biophysical Journal* **51**, 849–863.

MELZER, W., SCHNEIDER, M. F., SIMON, B. J. & SZÜCS, G. (1986). Intramembrane charge movement and calcium release in frog skeletal muscle. *Journal of Physiology* **373**, 481–511.

MILEDI, R., PARKER, I. & SCHALOW, G. (1977). Measurement of calcium transients in frog muscle by the use of arzenazo III. *Proceedings of the Royal Society* B **198**, 201–210.

MILEDI, R., PARKER, I. & SCHALOW, G. (1981). Calcium transient in normal and denervated slow muscle fibres of the frog. *Journal of Physiology* **318**, 191–206.

POTTER, J. D., JOHNSON, J. D., DEDMAN, J. R., SCHREIBER, W. E., MANDEL, F., JACKSON, R. L. & MEANS, A. R. (1977). Calcium-binding proteins: relationship of binding, structure, conformation and biological function. In *Calcium-binding Proteins and Calcium Function*, ed. WASSERMAN, R. H., CORRADINO, R. A., CARAFOLI, E., KRETSINGER, R. H., MACLENNAN, D. H. & SIEGEL, F. L., pp. 239–250. North-Holland, Amsterdam.

RAJU, B., MURPHY, E., LEVY, L. A., HALL, R. D. & LONDON, R. E. (1989). A fluorescent indicator for measuring cytosolic free magnesium. *American Journal of Physiology* **256**, C540–548.

ROBERTSON, S. P., JOHNSON, J. D. & POTTER, J. D. (1981). The time course of Ca^{2+} exchange with calmodulin, troponin, parvalbumin, and myosin in response to transient increases in Ca^{2+}. *Biophysical Journal* **34**, 559–569.

SIMON, B. J. & SCHNEIDER, M. F. (1988). Time course of activation of calcium release from sarcoplasmic reticulum in skeletal muscle. *Biophysical Journal* **54**, 1159–1163.

SMITH, J. S., CORONADO, R. & MEISSNER, G. (1986). Single channel measurements of the calcium release channel from skeletal muscle sarcoplasmic reticulum. *Journal of General Physiology* **88**, 573–588.

TSIEN, R. & POZZAN, T. (1989). Measurement of cytosolic free Ca^{2+} with Quin2. In *Methods in Enzymology*, vol. **172**, part S, ed. FLEISCHER, S. & FLEISCHER, B., pp. 230–262. Academic Press Inc., San Diego, CA, USA.